RELATIONSHIP BETWEEN RADAR LINEAMENTS, GEOLOGIC STRUCTURE, AND IN SITU STRESS IN EAST TEXAS

TOPICAL REPORT
(June 1987 - February 1988)

Prepared by
Robert W. Baumgardner, Jr.

Bureau of Economic Geology
W. L. Fisher, Director
The University of Texas at Austin
Austin, Texas 78713

for

THE GAS RESEARCH INSTITUTE
Contract No. 5082-211-0708
D'Arcy Horner, GRI Project Manager

March 1988

QAe7524

DISCLAIMER

LEGAL NOTICE. This report was prepared by the Bureau of Economic Geology as an account of work sponsored by the Gas Research Institute (GRI). Neither GRI, members of GRI, nor any person acting on behalf of either:

a. Makes any warranty or representation, expressed or implied, with respect to the accuracy, completeness, or usefulness of the information contained in this report, or that the use of any apparatus, method, or process disclosed in this report may not infringe privately owned rights; or

b. Assumes any liability with respect to the use of, or for damages resulting from the use of, any information, apparatus, method, or process disclosed in this report.

50272-101

REPORT DOCUMENTATION PAGE	1. REPORT NO. GRI-88/0093	2.	3. Recipient's Accession No.

4. Title and Subtitle
Relationship between radar lineaments, geologic structure, and in situ stress in East Texas

5. Report Date May 1988

6.

7. Author(s)
Robert W. Baumgardner, Jr.

8. Performing Organization Rept. No.

9. Performing Organization Name and Address
Bureau of Economic Geology
The University of Texas at Austin
University Station, Box X
Austin, Texas 78713

10. Project/Task/Work Unit No.

11. Contract(C) or Grant(G) No.
(C) 5082-211-0708
(G) (Gas Research Institute)

12. Sponsoring Organization Name and Address
Gas Research Institute
8600 West Bryn Mawr Avenue
Chicago, Illinois 60631
Project Manager:
D'Arcy Horner

13. Type of Report & Period Covered
Topical
June 1987 - February 1988

14.

15. Supplementary Notes

16. Abstract (Limit: 200 words)
Radar-based lineaments in East Texas and northwest Louisiana were studied to determine their relationship to surficial and subsurface geologic structure and to in situ stress. For all lineament data, two significant azimuths of vector sums were defined: 325° and 37°. The northwest trend has the same orientation as the mean direction of wellbore elongations in the Schuler Formation throughout the East Texas Basin. However, this trend is significantly different from the 344° orientation of wellbore elongation in the overlying Travis Peak Formation. These results suggest a complex relationship between subsurface stress and the northwest lineament trend. The northeast lineament trend does not coincide with the orientation of any known stress or regional structure and may be an artifact of radar illumination direction. Unlike a previous regional study based on smaller-scale Landsat data, no consistent correlation between surficial or subsurface structure and lineament density was discovered. However, high values of lineament density occur preferentially on outcrops of the Sparta and Weches Formations. These results suggest that either (1) most radar lineaments smaller than Landsat lineaments are manifestations of unmapped subregional or local structures or (2) most radar lineaments are surficial phenomena, unrelated either to subsurface geologic structure or to stress.

17. Document Analysis a. Descriptors
East Texas, lineaments, radar, remote sensing, stress

b. Identifiers/Open-Ended Terms
radar-based lineament study, analysis of stress directions based on stress tests, fractures and wellbore ellipticity

c. COSATI Field/Group

18. Availability Statement
Release unlimited

19. Security Class (This Report) Unclassified

21. No. of Pages 53

20. Security Class (This Page) Unclassified

22. Price

(See ANSI-Z39.18) *See Instructions on Reverse*

OPTIONAL FORM 272 (4-77)
(Formerly NTIS-35)
Department of Commerce

RESEARCH SUMMARY

Title	Relationship between Radar Lineaments, Geologic Structure, and In Situ Stress in East Texas
Contractor	Bureau of Economic Geology, The University of Texas at Austin, GRI Contract No. 5082-211-0708, entitled "Geologic Analysis of Travis Peak/Hosston and Corcoran-Cozzette Tight Gas Sandstones."
Principal Investigators	R. J. Finley, S. P. Dutton
Report Period	June 1987 - February 1988 Topical Report
Objective	This report describes the results of remote-sensing studies of an area in East Texas based on synthetic aperture radar (SAR) data. These results are compared with previous Landsat-based regional remote-sensing studies. The purpose of the study was to determine whether radar lineaments can be used to define in situ stress orientations in the Travis Peak Formation and thereby ascertain whether subsurface fracture orientation can be predicted from surface lineaments where subsurface stress data are absent in East Texas.
Technical Perspective	Previous remote-sensing studies of East Texas and northwestern Louisiana based on Landsat data showed that surface lineaments were subparallel to elongated structures in the subsurface and were parallel to minimum compressive stress in the Jurassic Schuler Formation. The current subregional study was conducted using SAR data from a small area of interest encompassing sites of wells drilled as part of ongoing research on the Travis Peak Formation. Given the low topographic relief of the study area, radar data were chosen for their ability to detect subtle topographic features. This report summarizes the results of lineament studies on the radar data and compares lineament orientations to orientations of in situ stress in the Travis Peak.
Results	Predominant radar lineament trends are very similar to Landsat-based lineament trends. However, radar lineament density does not delineate any mapped subsurface geologic structures. It is affected to some extent by surficial geology. Vector sums of lineament orientations are significantly different from those of in situ stress in the Travis Peak. The number of man-made features mistakenly identified as lineaments is higher for radar data than for Landsat data because man-made features are more visible on the higher-resolution radar imagery. This may also explain why lineament density is influenced by surface geology rather than by subsurface structure.
Technical Approach	Lineament studies were based on four 1:100,000-scale radar images. Lineaments were mapped on transparent overlays, checked against larger-scale photomosaics, digitized, and compiled as polar diagrams of statistically significant vector sums of lineament orientations. Lineament density was contoured using lineament length per unit area.

CONTENTS

FIGURES

TABLES

ABSTRACT

Radar-based lineaments in a 19,000 km^2 (7,400 mi^2) area of East Texas and northwest Louisiana were studied to determine their relationship to surficial and subsurface geologic structure and to in situ stress. For all lineament data, two significant azimuths of vector sums were defined: 325° and 37°. The northwest trend has the same orientation as the mean direction of wellbore elongations in the Schuler Formation throughout the East Texas Basin. However, this trend is subparallel to, and significantly different from, the 344° orientation of wellbore elongation in the overlying Travis Peak Formation. These results suggest a complex relationship between subsurface stress and the northwest lineament trend. The northeast lineament trend does not coincide with the orientation of any known stress or regional structure and may be an artifact of radar illumination direction. Unlike a previous regional study based on smaller-scale Landsat data, no consistent correlation between surficial or subsurface structure and lineament density was discovered. However, high values of lineament density occur preferentially on outcrops of the Sparta and Weches Formations. These results suggest that either (1) most radar lineaments smaller than Landsat lineaments are manifestations of unmapped subregional or local structures or (2) most radar lineaments are surficial phenomena, unrelated either to subsurface geologic structure or to stress.

INTRODUCTION

Purpose and Scope

The purpose of this investigation was to analyze surficial linear features and subsurface structure and stress in East Texas and northwest Louisiana (fig. 1) and to answer two questions. First, can the correlation between surface lineaments and subsurface structure and stress that was demonstrated on a regional basis in a previous study (Baumgardner, 1987) be detected at a subregional level? Second, how are surficial linear features related to geologic structure and subsurface stress in the study area? This area was selected as part of an analysis of the Cretaceous Travis Peak (Hosston) Formation, a low-permeability, gas-bearing sandstone, which does not crop out in the study area. Because fracture permeability in the Travis Peak is a significant part of its total permeability, the orientation of fractures strongly controls the direction of gas movement. Knowing the orientation of those fractures will be an essential part of any plan to produce the formation's gas resources. Subsurface fracture orientation sometimes can be inferred from surface features (Verbeek and Grout, 1984). Surface lineaments and subsurface features are examined in this report using airborne synthetic aperture radar (SAR) data and subsurface data from seven wells. SAR data have higher resolution than the Landsat data used in the previous study. The subsurface data comprise ellipticity logs, fracture data, and strain relaxation data, all of which provide more detailed information about subsurface in situ stress than was available for the regional study.

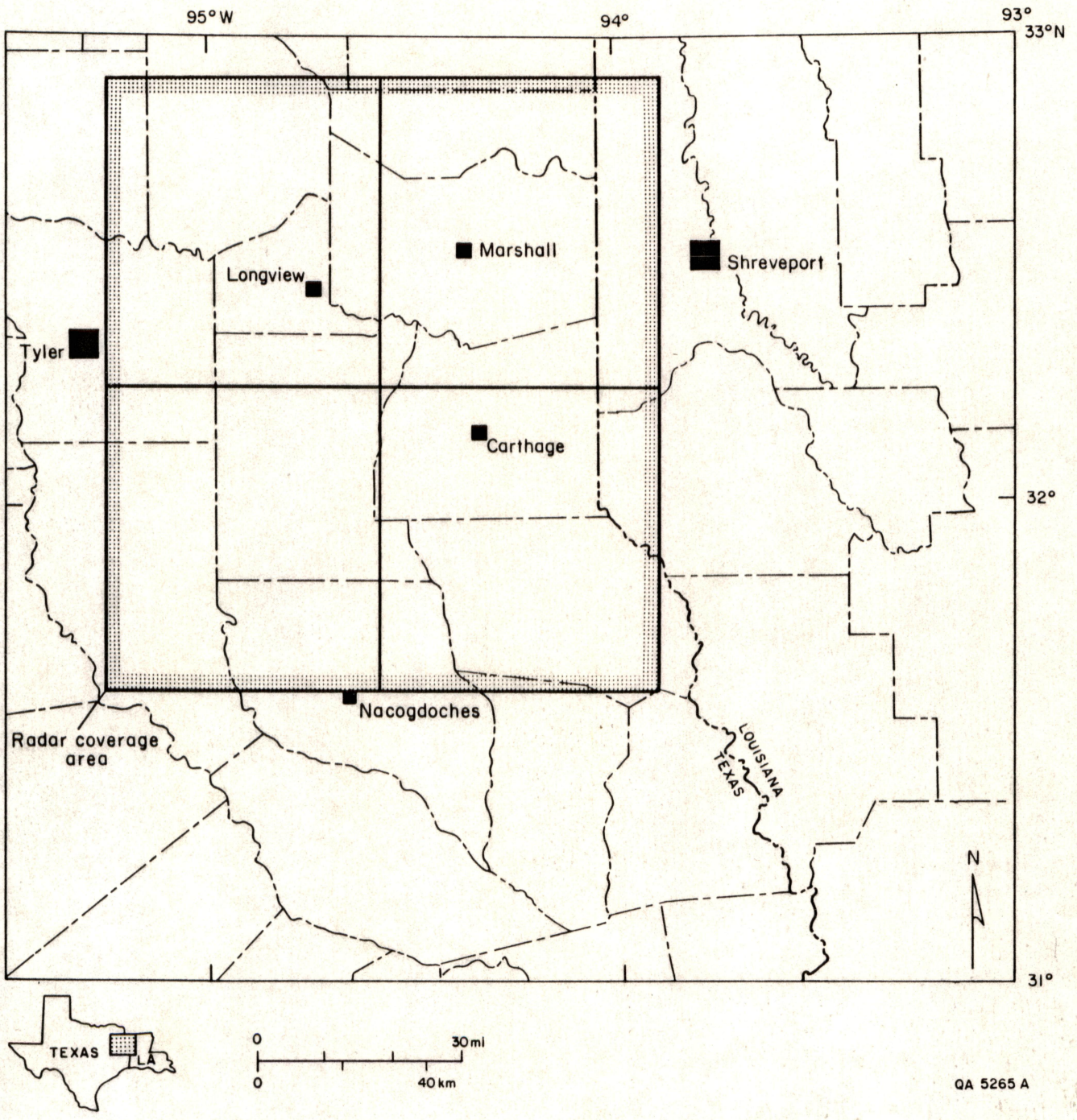

Figure 1. Location of study area and four radar mosaics in East Texas and northwest Louisiana. Original scale of radar mosaics was 1:100,000. Each of the four images is referred to by the name of the town shown on or within its borders.

Previous Work

Other workers have investigated the relationship between linear features on the Earth's surface, such as fractures, and subsurface geologic structure (Berger, 1982; Tillman, 1983; Bailey and others, 1984; Woodruff and Caran, 1984). Perhaps more relevant to this study is the comparison of linear or elongated features in the subsurface with those at the surface. Hickman and others (1985) found wellbore elongations at right angles to the direction of natural fractures in the subsurface. The fractures were parallel to joints mapped at the surface. Komar and others (1971) studied surface features and vertical fractures in the subsurface in an area of flat and gently dipping rocks. They found vertical fractures in the subsurface subparallel to lineaments. However, subsurface fractures were nearly perpendicular to surface fractures. Baumgardner (1987) found elongated salt structures in the subsurface subparallel to lineaments and wellbore elongations parallel to lineaments.

Judging from these different studies, the relationship between orientations of linear features at the Earth's surface and in the subsurface is not the same everywhere. Indeed, in an area of complicated fracturing, Grout and Verbeek (1985) showed that surface and subsurface fractures can be either parallel or perpendicular in the same sedimentary basin because of differences in lithology and burial and thermal histories of the rocks involved. The comparatively simple geologic history of the study area indicates that such complexities are probably not present here. Nevertheless, the relationship between surficial and subsurface linear features is not always straightforward.

Lineaments, because they are physiographic features, are assumed to be manifestations of geologic structure or stress. The mechanism by which they form

is not well understood, because the lineaments themselves usually are not identified as fractures, joints, or fault traces, whose origins are reasonably well documented. Although the history of development of fractures, joints, or faults at a given location may be complex, their mechanical development is evident: the rock is broken and, in the case of faults, displaced. The size and diffuse boundaries of lineaments often preclude such recognition. A lineament may be a valley formed along an unrecognized fault trace, or it may be a line of hills where erosion is controlled by a jointing pattern that is obscured by vegetation. Whatever the case may be, the mechanical origin of a lineament is difficult to determine precisely because it usually cannot be identified as a specific geologic feature.

METHODS AND MATERIALS

Synthetic Aperture Radar

Synthetic aperture radar (SAR) data were used in this study because they can reveal subtle topographic, and presumably, structural features. The utility of these data has been proven in studies of geologic structure in tropical areas where thick vegetation or persistent cloud cover limits the use of other sensors (Sabins, 1986). The long wavelength of X-band radar (2.4 to 3.8 cm, or 0.9 to 1.5 in) allows it to penetrate clouds and, to some extent, dry soils, both of which block most shorter wavelengths (Trevett, 1986). Radar imaging is primarily a method for detecting surface roughness. Distracting differences between similar kinds of vegetation that can obscure geologic structure on other image types are subdued in radar data. However, substantial differences in vegetation cover, such as between trees and grassland, are detected.

Because it is an active sensor, generating its own signal and receiving a reflected pulse in return, SAR is a highly flexible tool. The depression angle and direction of illumination of the radar signal can be adjusted to meet different requirements of terrain roughness and structural trends (fig. 2). Near-range data, that part of the ground swath closest to the airplane and the radar antenna, have the steepest depression angle (14.4° to 37.7°, fig. 2) and the shortest shadows. Far-range data, farthest from the antenna, have the shallowest depression angle (8.8° to 14.4°, fig. 2) and the longest shadows.

The data for this study were radar mosaics constructed from individual flight-line strips. This allowed us to select the part of the original data strips that best suited our purposes. Because low topographic relief predominates in the study area, far-range data were selected for construction of the mosaics. Average depression angle for the radar mosaics in this study is 11°. Terrain slopes vary from less than 1° to 14°, as measured on 1:250,000-scale topographic maps of the region. Therefore, Yamaguchi's (1985, p. 126) condition for radar shadowing has been met: "The most fundamental condition for radar shadow enhancement is that the range of radar depression angle [sic] overlaps with the range of angles of terrain slopes." Otherwise, no radar shadows are formed.

Just as depression angle can be adjusted, so can direction of illumination. The direction that the radar beam is aimed can optimize radar shadows. MacDonald and others (1969) reported that for optimum enhancement, the illumination direction should be perpendicular to the target. Wise (1969), on the other hand, concluded that optimum shadow enhancement of a valley wall depends on the slope of the valley wall and the radar depression angle:

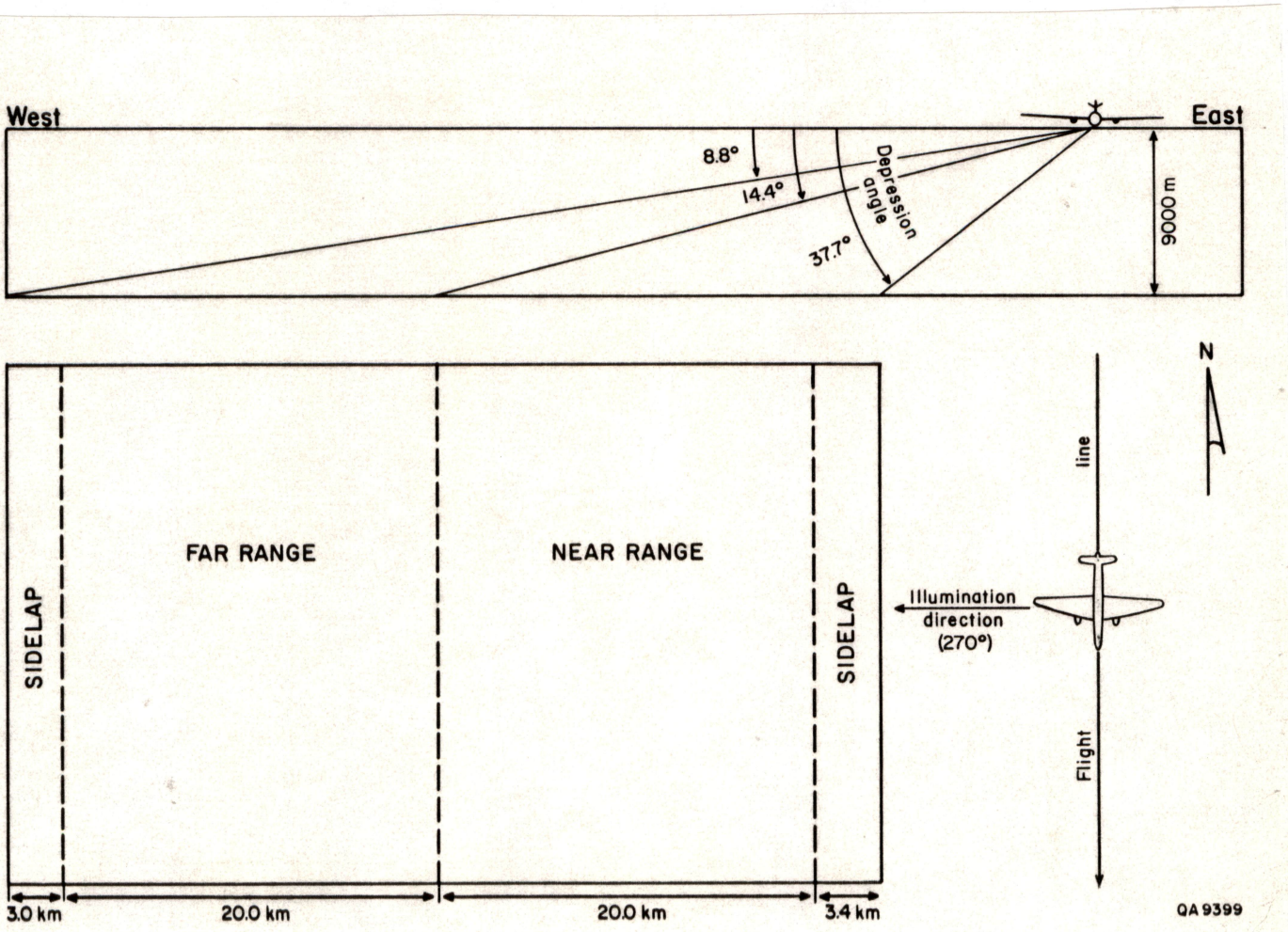

Figure 2. Method of collecting airborne radar data used in this study. Far-range data, with an average depression angle of 11° (below horizontal), were used to construct mosaics. Direction of illumination was 270°. Modified from INTERA Technologies (1985, fig. 1).

$$\sin \alpha = \tan \beta / \tan \chi \quad (1)$$

where α = angle between trend of valley and radar illumination

β = radar depression angle

χ = slope of valley wall

Radar illumination direction is 270° for the data in this study. The depression angle for far-range data ranges from 8.8° to 14.4° (fig. 2). Slopes of valley walls in East Texas are mostly less than 14°. Consequently, optimum shadow enhancement of valley walls will occur from 270°$\pm$38° to 270°$\pm$90°--that is, from 308° to 360° and from 360° to 52°. (The interval from 360° to 52° is equivalent to the interval from 180° to 232°. All directions in this report are referred to using the northern half of the compass: 270° to 0° to 90°.). This is a very broad range, covering an arc 104° wide from 308° to 52°. If the average radar depression angle of the data (11°) is used in equation 1, two narrower zones of shadow enhancement result: 321° to 352° and 8° to 39°.

In this study, as recommended by Cannon (1982), the radar illumination direction is at a high angle to the illumination direction of Landsat data available for the area (table 1). The purpose of this difference in illumination direction is to enhance any features with different orientations that were not detected on Landsat imagery examined in a previous remote-sensing study of the area (Baumgardner, 1987).

Because these radar data are being used in conjunction with Landsat thematic mapper (TM) data, it is instructive to compare the two data types (table 1) and their effect on lineament mapping. The scale of the Landsat data was 1:250,000, 2-1/2 times smaller than the scale of the SAR data (1:100,000). Resolution of the radar data is 6 by 12 m (20 by 40 ft) (INTERA Technologies, 1985), compared with 30 by 30 m (98 by 98 ft) for Landsat TM data. The individual picture elements

Table 1. Comparison of Landsat thematic mapper (band 5) and synthetic aperture radar (SAR) (X-band) remote-sensing data available for the study area. Direction and angle of illumination for Landsat data vary because four different images were used to cover the region.

Characteristic	Landsat	SAR
Scale	1:250,000	1:100,000
Resolution (m)	30 x 30	6 x 12
Direction of illumination	321°-330°	270°
Wavelength	1.55-1.75 μm	2.4-3.8 cm
Illumination/depression angle	31°-35°	11°
Maximum lineament length (km)	72.3	17.6
Minimum lineament length (m)	290	290
Mean lineament length (m)	3,500	1,500

(pixels) of the SAR data are about 1/12 the size of the Landsat pixels. Consequently, many features between 6 and 30 m (20 and 98 ft) wide that cannot be detected by the Landsat TM are visible on the radar images.

The wavelengths of electromagnetic energy detected by the two sensors are quite different. Consequently, they will detect different features or will represent the same features differently. Band 5 (mid-infrared) of the Landsat TM data covers the range from 1.55 to 1.75 μm. At these wavelengths, differences in moisture content of soils and vegetation are visible. Wavelength of X-band radar is much longer, ranging from 2.4 to 3.8 cm (0.9 to 1.5 in) (Sabins, 1986). At this wavelength, the radar can detect differences in surface roughness in the range of a few centimeters. No return signal is received from horizontal, smooth surfaces, such as lakes, which reflect all the incident radar energy away from the antenna. However, rough surfaces scatter incident energy at all angles and give strong radar returns. The depression angle of the radar signal is a factor in the definition of a rough surface (Peake and Oliver, 1971). As depression angle decreases, the vertical relief required to define a rough surface increases:

$$h > \lambda/(4.4 \sin \beta) \qquad (2)$$

where h = vertical relief

λ = wavelength of the radar

β = radar depression angle

For the radar data used in this study, where average β=11° and λ=2.4 to 3.8 cm (0.9 to 1.5 in), a rough surface has vertical relief (h) greater than 2.9 to 4.5 cm (1.1 to 1.8 in). It is unlikely that any surfaces in the study area, except surfaces of water bodies, have vertical relief less than 4.5 cm (1.8 in), so strong returns would be expected from all surfaces. Because of the variable land cover in the study area, most of the difference in radar signal return is caused by reflection

from much larger features, such as trees, not by differences in roughness of the ground surface or of a uniform leaf canopy in a forest. Strongest signals are received from corner reflectors, such as steeply sloping riverbanks, edges of clear-cut areas in woods, and buildings, all of which return the energy directly to the antenna.

Lineament Mapping

The definition by Woodruff and Caran (1984, p. 8) is used to describe lineaments in this study: "A pattern of tones, textures, contours, and other such features that is straight, linear, and . . . continuous, has definable end points and lateral boundaries (high length/width ratio), and hence a discernible azimuth."

Lineaments were mapped on four radar image mosaics at 1:100,000-scale in four steps. First, the radar image was placed on a light table and viewed with transmitted light in a darkened room. A transparent sheet of mylar was placed over the image, and the end points of each lineament were marked. Second, after thorough visual inspection was complete, a second sheet of transparent mylar was placed over the first, and the end points were connected by a line drawn on the second sheet. In this way the image was not obscured during the initial visual inspection by a growing network of lines. Third, the mapped lineaments were checked against larger-scale photomosaics (1:63,360-scale) and, when available, aerial photographs (1:20,000- and 1:40,000-scale). Lineaments were copied from the second mylar overlay onto the photomosaics using a proportional projector to enlarge the lineament overlay to the scale of the photomosaics. At this point in the procedure lineaments were described (table 2), and those corresponding to man-made features were erased from the overlay. Fourth, the lineaments remaining after the removal of

Table 2. Descriptions of lineaments identified on large-scale aerial photographs and photomosaics. Lineaments in Louisiana (fig. 3) are not included in this table.

Description	Number	Percent
Straight valley	288	30.1
Sinuous valley with straight plan view	214	22.4
Sinuous stream with straight plan view	139	14.5
Straight edge of lake	82	8.6
Straight reach of meandering river/valley	69	7.2
Straight ridgetop, valley wall	22	2.3
Straight meanderbelt/floodplain	17	1.8
Straight abandoned meander, swale	17	1.8
Straight stream	14	1.5
Dentate ridge with straight plan view	7	0.7
Channels aligned across valley/divide	6	0.6
Vegetation boundary	5	0.5
Unidentified	77	8.0
Total	957	100.0

man-made features were digitized. Lineaments from all images were compiled into one data set for display and analysis (fig. 3).

Lineaments that were neither man-made nor clearly associated with some natural feature, such as a straight stream valley, were not erased. These were usually mapped on straight tonal boundaries that were visible on the radar images but were not apparent on the larger-scale photographs.

To ensure that each mosaic was given equally rigorous inspection during the first step of lineament mapping, records were kept of time spent studying each mosaic. Each scene was examined for 5.9 to 7.1 hours (table 3). Differences in time spent examining each image were caused by differences in contrast on each one, but this did not significantly affect mapping of lineaments. This inspection phase included a period during which discrete parts of the image were viewed for a fixed time. A mask was placed over the mosaic and 1/9 of the scene was studied for 10 minutes. During this step all parts of the radar image received equal attention.

No significant correlation (positive or negative) exists between amount of time spent per image and number of lineaments detected (table 3). Fewer lineaments were detected on the Marshall image (fig. 1), which was studied longer than any of the others (table 3). The difference in number of lineaments detected may be due to differences in vegetation cover throughout the area, but this remains unproven.

The percentage of man-made features erroneously mapped as lineaments increased six-fold compared with those mapped in the previous Landsat-based study. Erroneous lineaments amounted to 22.2 percent of all lineaments mapped from radar data (table 3) but only 3.7 percent of those mapped from Landsat images (Baumgardner, 1987). Half of these man-made features are boundaries between woods and cleared land (table 4). A third are roads. Apparently, many of these features are too small (less than 30 m wide) to be detected by the Landsat TM but are visible on the higher-resolution SAR images. After these man-made features were

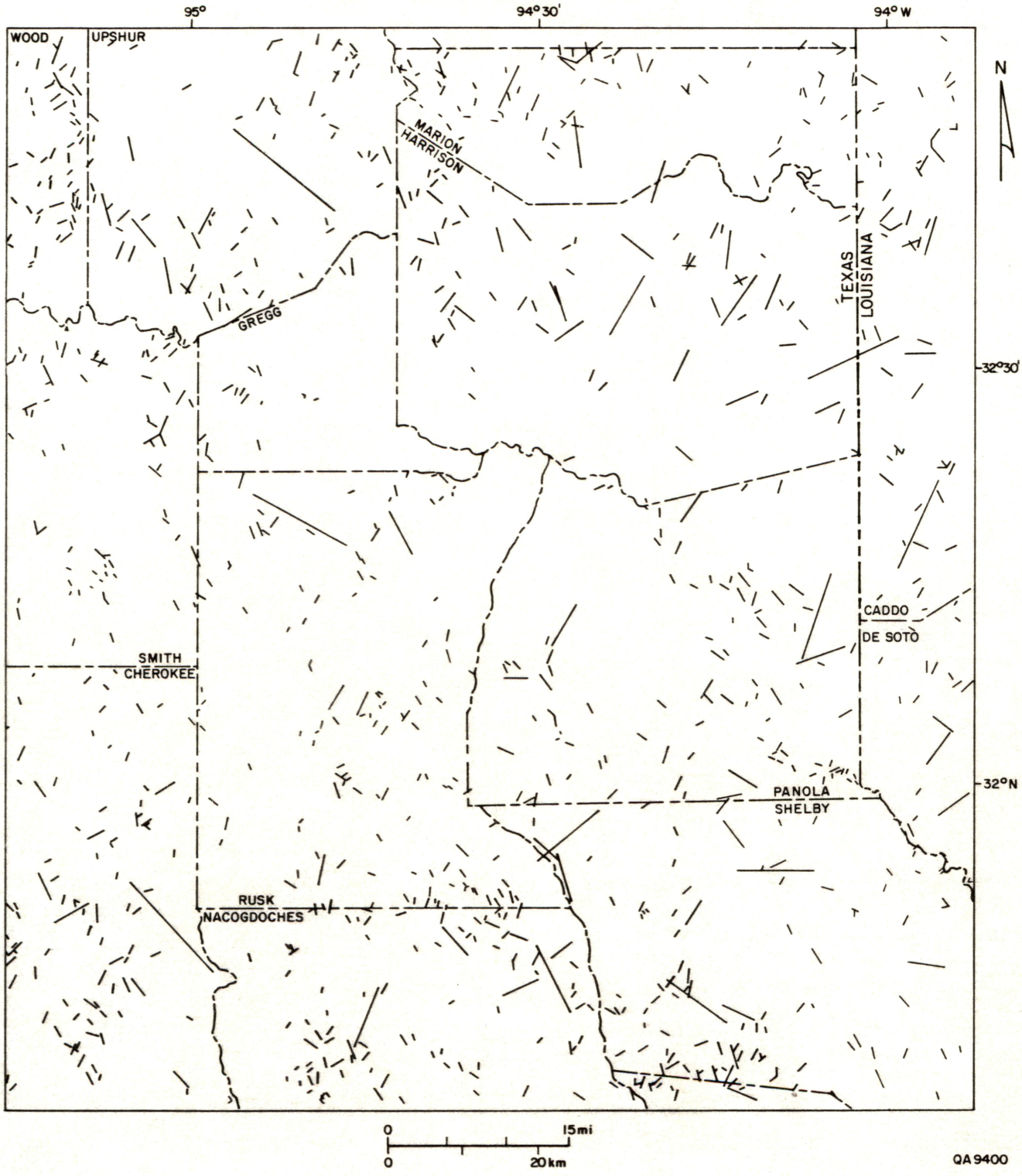

Figure 3. Map of radar-based lineaments in this study. See figure 1 for location of study area.

Table 3. Results of mapping lineaments on four radar images. Lineaments were checked against larger-scale aerial photographs and photomosaics to eliminate man-made features. The number of correct lineaments is less than the total number in the study because some lineaments could not be checked against photographs or photomosaics. See figure 1 for location of images and figure 3 for map of lineaments.

Image name	Mapping time (hr)	Number of lineaments			Error (%)
		Checked	Correct	In error	
Carthage	5.9	319	248	71	22.3
Longview	6.2	361	284	77	21.3
Marshall	7.1	179	142	37	20.1
Nacogdoches	6.0	372	283	89	23.9
Total	25.2	1231	957	274	22.2

Table 4. Descriptions of features erroneously mapped as lineaments. These features were deleted from the lineament maps before digitizing and were eliminated from further analysis of lineament data.

Description	Number	Percent
Boundary between woods/cleared land	138	50.3
Road	92	33.5
Other cut vegetation boundary	12	4.4
Fence/property line	8	2.9
Powerline, pipeline, firebreak	7	2.6
Railroad	4	1.5
Straightened edge of lake	4	1.5
Straightened channel	4	1.5
Other	5	1.8
Total	274	100.0

removed from maps of lineaments, more than 1,000 lineaments remained for further study.

Compilation of Orientation Data

Orientations of the lineaments and wellbore ellipticity were displayed as polar diagrams of length-weighted frequency (F) following the procedure outlined by Dix and Jackson (1981). To avoid the graphical exaggeration of large values inherent in polar plots (because the area of each sector increases in proportion to the square of its length), the square roots of F values were plotted (fig. 4a).

A sector width of 10° (0° to 9°, 10° to 19°, and so forth) was used. The choice of sector width within the polar plot may arbitrarily limit the number of significant peaks of orientation data. For example, a large F value may be divided between two adjoining sectors, thereby obscuring what otherwise would have been a significant peak.

Calculating vector sums of adjacent peaks prevents this loss of data. Adjacent sectors larger than the mean value of F are summed and the resultant vector is plotted (fig. 4b). As an added refinement, a chi-square test is applied to each vector to determine its level of significance (Vistelius, 1966; Dix and Jackson, 1981). The resultant value, known as the Bernshtein accuracy criterion (H), is plotted with the same azimuth as the vector sum (fig. 4c). The 99-percent confidence level is used to define significant sector peaks. Dix and Jackson (1981) showed that sector peaks significant at the 95-percent confidence level could be obtained with synthetic "lineaments" derived from a random-number table, but the 99-percent confidence level was high enough to exclude randomly generated peaks where large data sets were used.

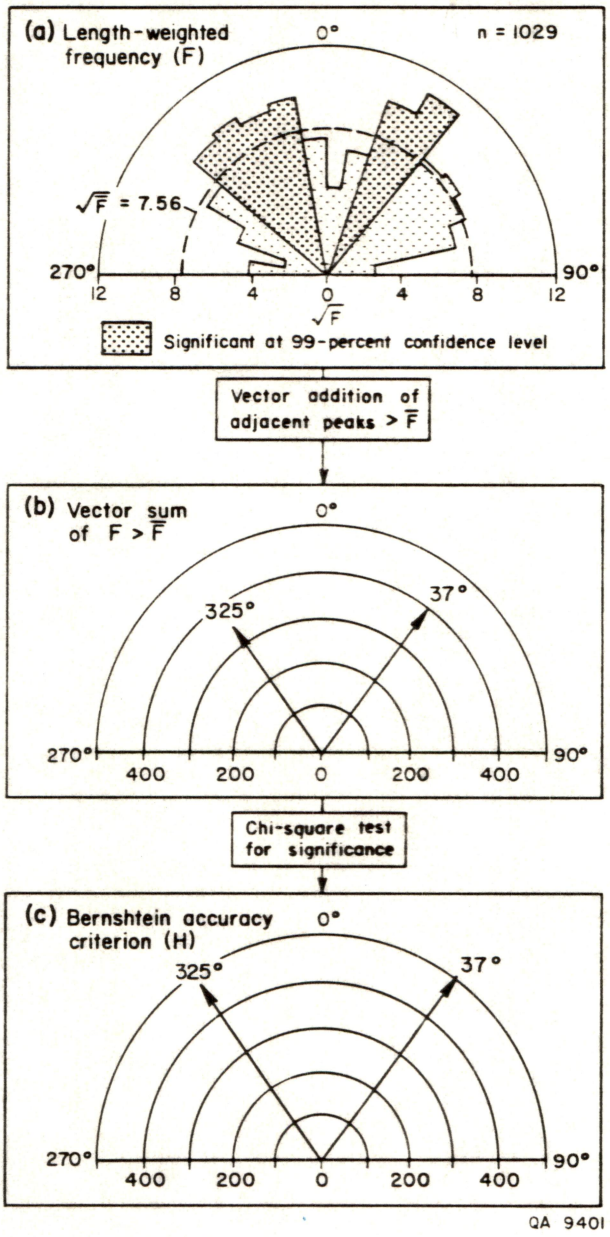

Figure 4. Procedure for statistical evaluation of orientation data. Polar graphs of orientation data are generated by summing lineament length for each sector of the graph. These data represent 1,029 radar-derived lineaments. The same procedure is used to determine significant orientations of wellbore ellipticity. (a) Length-weighted frequency (F) of lineaments has six sectors significant at the 99-percent confidence level. The square root of F is plotted to prevent areal exaggeration of large peaks. (b) Adjacent peaks larger than the mean value of F, when combined by vector addition, produce only two significant peaks. (c) Two peaks of Bernshtein accuracy criterion (H) are significant at the 99-percent confidence level, based on a chi-square test.

Small data sets, however, may include statistically significant orientation peaks that are not valid. Dix and Jackson (1981) found that data sets of synthetic "lineaments" with fewer than 200 values contained peaks that were significant even at the 99-percent confidence level. As a result, they recommended that lineament data sets have at least 200 values to avoid including spurious peaks. In this study, the total number of radar lineaments (1,029) exceeds the minimum recommended by Dix and Jackson (1981).

Significant lineament orientations were carefully determined in order to compare them with the orientations of principal stresses and fractures in the subsurface. These results were then compared with the relationship between stress and fracture orientations reported by other workers (Komar and others, 1971; Grout and Verbeek, 1985; Hickman and others, 1985). Stress direction is examined in the following section.

Defining Principal Stress Directions

The orientation of least principal horizontal stress can be defined by, or deduced from, several kinds of data. In this study, four data sets were available for determining the direction of least principal horizontal stress: (1) anelastic strain analysis tests, (2) differential strain curve analysis (DSCA), (3) orientations of natural and man-made fractures, and (4) orientations of wellbore elongations. Because only the wellbore elongation data set is large enough to meet the minimum size requirement (200 data values) recognized by Dix and Jackson (1981), the mean vector sum of the other oriented features was calculated (Cheeney, 1983; Davis, 1986). The procedure is somewhat different from that of Dix and Jackson (1981) in that there is no length associated with strain analysis or with fractures. Mean orientation is a measure of orientation but not length.

The amount of scatter in the orientation is expressed by the mean resultant length ($\bar{R}$) (table 5). $\bar{R}$ values close to 1.0 (the maximum value) indicate low scatter. All values of $\bar{R}$ in table 5 are significant at the 99-percent confidence level. Consequently, we reject the null hypothesis that there is no preferred trend to these features.

Strain Analysis

Recent work in the Holditch Howell No. 5 well (fig. 5) provides information about stress relations in southeastern Harrison County, Texas. We calculated mean vector sum azimuth of the maximum principal horizontal stresses reported by Owen and others (1987). It is $77° \pm 33°$ at the 99-percent confidence level (fig. 6a), based on six "excellent" measurements of anelastic strain recovery from core samples (table 5). On the basis of these data, minimum horizontal stress has an average azimuth of $347° \pm 33°$, perpendicular to the maximum horizontal stress. Differential strain curve analysis carried out on a single core sample from the same well (Jeffrey and others, 1987) yielded stress orientations that generally confirm this conclusion. On the basis of the results of that test, we calculated mean vector sum of maximum principal horizontal stress. It has a mean orientation of $86° \pm 8°$ at the 99-percent confidence level (fig. 6b).

Fracture Orientations

The predominant trend of natural and coring-induced fractures in the Travis Peak Formation is east-northeast to east (Laubach and others, 1987, figs. 3, 4). Because the study area is in a region of extensional stress (Zoback and Zoback, 1980, fig. 5) these are presumably tension fractures, oriented perpendicular to the

Table 5. Orientations of maximum horizontal principal stress (Hmax) in the East Texas study area defined by various methods. The high values (approaching 1.0) of mean resultant length ($\bar{R}$) indicate that orientations are significant at the 99-percent confidence level. Number of wellbore elongations includes only those composing the significant northeast peak.

Feature/Test	Number	Orientation of Hmax	$\bar{R}$	Source of data
Anelastic strain recovery	6	77°±33°	.86	Owen and others, 1987
DSCA* test	15	86°±8°	.98	Jeffrey and others, 1987
Fractures	41	87°±11°	.90	E. R. Monson, personal communication, 1987
Wellbore elongation	196	74°±2°	.92	This study

*DSCA=Differential strain curve analysis

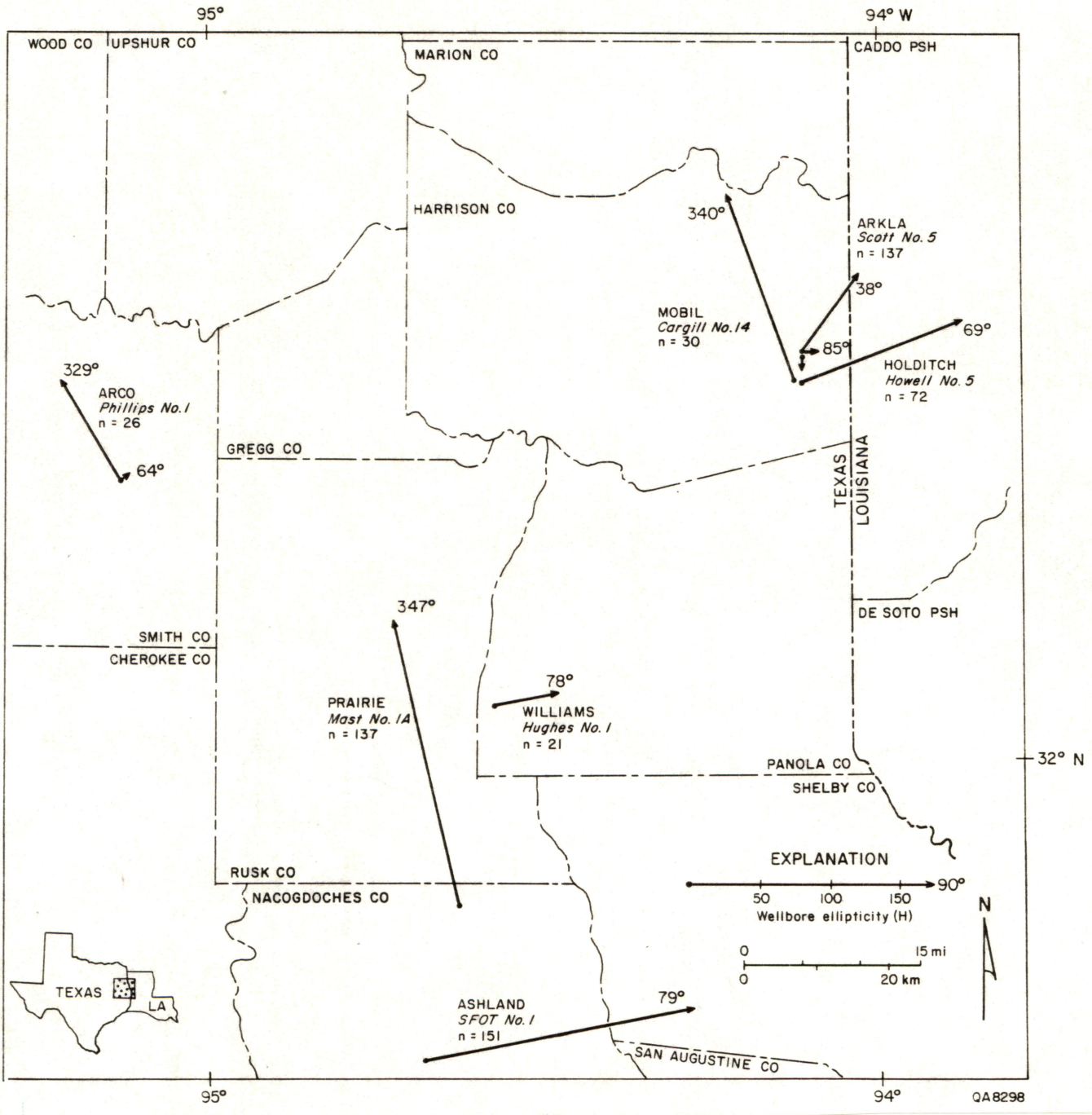

Figure 5. Map of seven wells with polar plots of wellbore ellipticity. Orientations of vector sums in adjacent wells are approximately perpendicular.

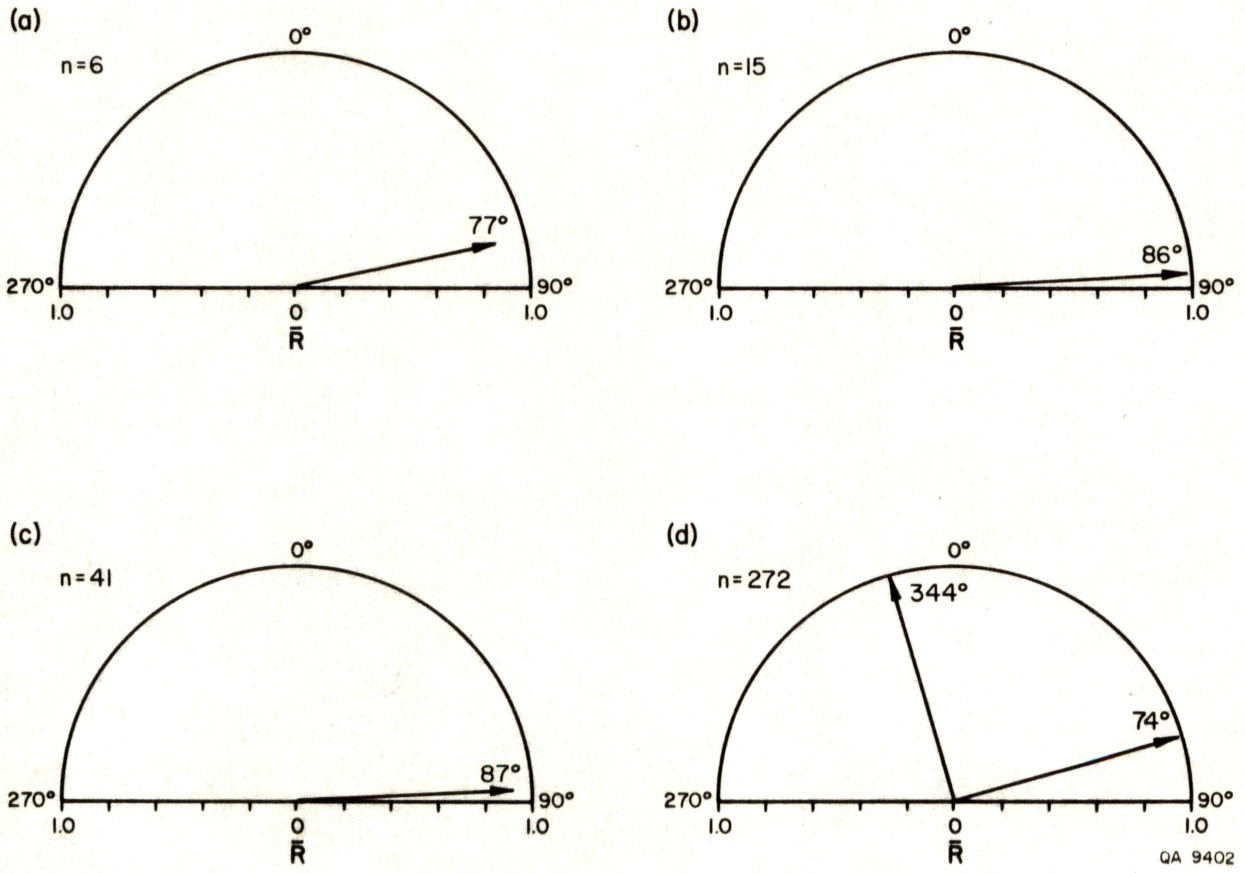

Figure 6. Polar plots of stress-related phenomena. All values of mean resultant length ($\bar{R}$) are significant at the 99-percent confidence level. (a) Mean orientation of maximum horizontal stress based on strain recovery tests is $77° \pm 33°$. (b) Mean orientation of maximum principal horizontal stress based on differential strain curve analysis is $86° \pm 8°$. (c) Mean orientation of maximum horizontal stress based on fracture orientations is $87° \pm 11°$. (d) Significant vector sums of wellbore elongations are $344° \pm 1°$ and $74° \pm 2°$. Northwest trend is orientation of wellbore breakouts formed by spalling under in-situ stress conditions. Northeast trend is orientation of tension fractures. Both trends indicate that maximum horizontal stress is oriented $74° \pm 2°$. Number of wellbore elongations includes only those composing the two significant peaks.

azimuth of minimum horizontal stress and opening against the least principal horizontal stress. The mean vector sum of 41 fractures from 4 wells in the study area (Cargill No. 14, Howell No. 5, Hughes No. 1, and Mast No. 1A, fig. 5) has an orientation of 87°±11° at the 99-percent confidence level (table 5, fig. 6c). This is essentially the same as the azimuth of maximum horizontal stress based on data from Jeffrey and others (1987) and gives an orientation of minimum horizontal stress of 357°±11°.

These results of fracture orientation analysis should be interpreted with caution because only a few fractures are available for analysis. However, the consistent results from these and other data indicate that most fracture orientations are reliable indicators of stress orientations.

Wellbore Elongations

Wellbore elongation has been studied as a means of determining the orientations of horizontal principal stresses. Previous work by Plumb and Hickman (1985) distinguished between elongations caused by intersection of the wellbore with natural fractures and those caused by spalling of the wellbore (breakouts) in a stress field with unequal horizontal stresses. These results, as well as recent work by Gough and Bell (1982) and Zoback and others (1985), show that breakouts develop parallel to the minimum horizontal principal stress.

Data from a previous study of 50 wells scattered throughout East Texas provide important information about regional stress directions. Brown and others (1980) measured the azimuths of wellbore elongations in the Schuler Formation (which underlies the Travis Peak Formation) at depths below about 2,800 m (9,200 ft). Mean elongation azimuth for all wells was 325°. On the basis of orientations of

vertical hydraulic fractures (east-west) (Strubhar and others, 1975) and recently active normal faults (northeast-southwest) in the area, Gough and Bell (1982) concluded that the northwest orientation of these elongation azimuths was parallel to the least principal stress. This orientation is generally consistent with that derived independently from fracture data and strain analysis.

To obtain detailed information about wellbore elongation in the study area, well logs from seven wells were examined. As described in a recent report (Baumgardner and Meador, 1987), zones of wellbore elongation were measured on ellipticity logs produced by ResTech, Inc.

A total of 575 elliptical zones were detected (table 6). Data from each well were used to define significant directions of wellbore elongation (fig. 5). To define a value of significant wellbore ellipticity, the number, length, and azimuth of elliptical zones were analyzed using the same technique that was applied to the lineament data.

Most results from individual wells are clustered between 329° and 350° or between 64° and 85° (fig. 5). However, no single well contains enough elliptical zones to exceed the minimum value (200) recommended by Dix and Jackson (1981), so all data from all wells were analyzed together. For all data combined, two significant vector sums of wellbore ellipticity were found at right angles to each other: $344° \pm 1°$ and $74° \pm 2°$ (fig. 6d). On the basis of the fracture data and results of strain analysis tests, we conclude that the northwest ellipticity trend is parallel to least principal horizontal stress, and the northeast trend is parallel to tension fractures in the wellbores.

Table 6. Wellbore ellipticity data from seven wells in East Texas. Bernshtein accuracy criterion (H) shows the azimuth and magnitude of vector sums of elliptical zones. For location of wells see figure 5.

Well Name (Owner-Lease)	Number	H Az.	H Mag.
ARCO Phillips #1	27	329°	85
" "	"	64°	7
Arkla Scott #5	137	38°	74
" "	"	85°	13
Ashland SFOT #1	151	79°	199
Holditch Howell #5	72	69°	125
Mobil Cargill #14	30	340°	146
Prairie Mast #1A	137	347°	210
Williams Hughes #1	21	78°	48
All data	575	74°	229
" "	"	344°	101

Summary

The four techniques for determining stress orientations have given consistent results (table 5). Differential and anelastic strain analyses indicate that orientation of maximum principal horizontal stress is 77°±33° or 86°±8°. These orientations are not significantly different at the 99-percent confidence level. Fracture data and measurements of wellbore ellipticity show that maximum principal horizontal stress has an azimuth of 87°±11° or 74°±2°. These orientations overlap slightly but are significantly different at the 99-percent confidence level. The similarity of these independent measurements is convincing evidence that orientation of the least principal horizontal stress is well defined by these methods, given the level of accuracy of the original orientation measurements made on the core and on the ellipticity logs. The relationship between orientations of lineaments and stress is discussed in the following section.

RESULTS

Lineament Orientations

For all radar lineaments in the study area, two azimuths of H values are significant at the 99-percent confidence level: 325°±2° and 37°±2° (fig. 4c). These orientations are strikingly similar to those resulting from a Landsat-based study of lineaments in this region. The azimuths of H values for 2,250 lineaments examined in that study were 325° and 21° (Baumgardner, 1987, fig. 7c). Furthermore, the significant azimuths of only those Landsat lineaments in the radar study area that are within the size range of radar lineaments (290 m to 17.6 km, or 950 ft to 10.9 mi)

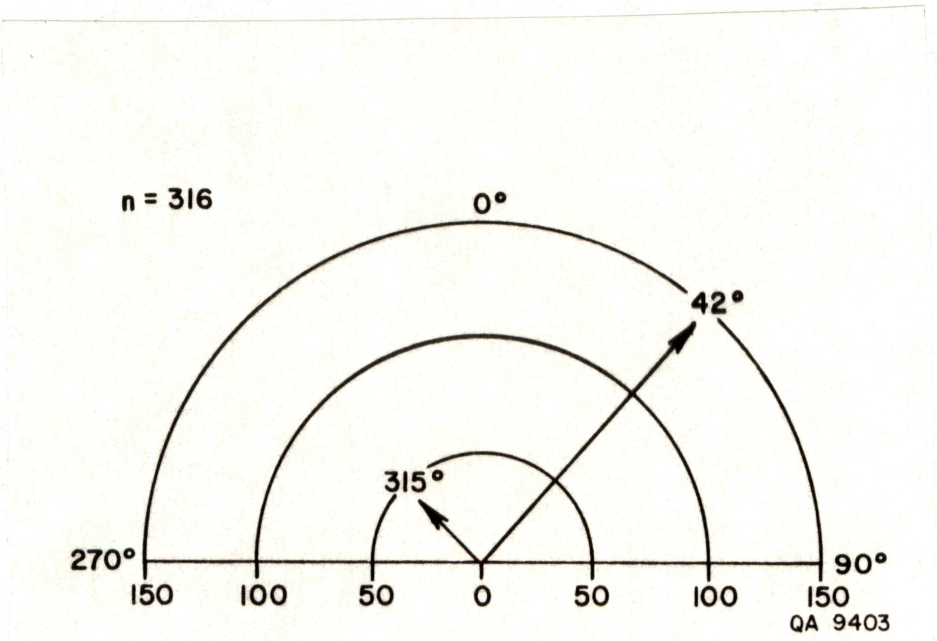

Figure 7. Polar plot of Bernshtein accuracy criterion (H) for Landsat-based lineaments in the study area. Only Landsat lineaments within the size range of radar lineaments (290 m to 17.6 km, or 950 ft to 10.9 mi) are included in this figure. The two peaks have orientations that are similar to those of radar-based lineaments (fig. 4c), but the northwest Landsat lineament peak is much smaller than the northwest radar lineament peak.

are 315° and 42° (fig. 7). These similarities between orientations derived from different sources are important given the differences between the two data sets.

Differences in scale and resolution produce a large difference in the size of lineaments detected. Length of radar lineaments ranges from 290 m to 17.6 km (950 ft to 10.9 mi) (table 1). Mean length of radar lineaments is 1,500 m (4,900 ft). Landsat lineaments vary from 290 m to 72.3 km (950 ft to 45.2 mi) in length, and their mean length is 3,500 m (11,500 ft).

Perhaps the most important difference between the data sets for the present study is the direction of illumination (table 1). Based on Wise's (1969) work, optimum shadow enhancement of valley walls in this study should occur between 321° and 352° and between 8° and 39°. Results show a close correspondence between these predictions and observed radar lineament orientations. Straight valleys compose about 30 percent of all lineaments in this study (table 2). Groups of 10°-wide sectors larger than the mean F value extend from 310° to 349° and from 20° to 69° (fig. 4a). However, it is not entirely clear that those orientation peaks are merely functions of radar illumination direction. The peaks overlap with the predicted zones of preferential radar shadowing, but the fit is imperfect. The radar peaks are composed of 10°-wide sectors that cover an arc wider than the zones predicted by Wise's (1969) work, and their boundaries do not exactly coincide with those predicted by theory (fig. 4a). In addition, the northwest peak seen in regional Landsat data (325°) (Baumgardner, 1987) is statistically equivalent to that seen on the radar imagery examined in this study (325°), based on an F-test of the two directional vectors (Davis, 1986). This concurrence represents two different sensors detecting the same regional and subregional trend in lineament orientation. The similarity is especially significant, given the differences of scale, resolution, wavelength, and angle and direction of illumination between the two data sets (table 1). Furthermore, it

suggests that the northwest radar lineament peak is not merely an artifact of the direction of radar illumination.

The relationship between the 325° orientation of lineaments and wellbore elongations is not consistent everywhere. It is parallel to the mean azimuth of wellbore elongations in the Schuler Formation throughout East Texas (Brown and others, 1980). This evidence suggests that the 325° lineament orientation is a manifestation of regional stress. However, the difference between northwest orientations of lineaments and wellbore breakouts in the Travis Peak Formation (344°) suggests that lineaments are not the results of in situ stress in the study area. These two orientations are significantly different at the 99-percent confidence level. Thus, the orientations of lineaments and wellbore elongations are not drawn from the same population, and there is very little chance that the lineament trend reflects the stress trend that results in wellbore breakouts. The geographic distribution of wells in which the northwest elongations predominate may account for this difference. Two wells on the uplift (Cargill No. 14 and Mast No. 1A, fig. 5) have azimuths oriented 340° and 347°, respectively. One well near the western edge of the study area (Phillips No. 1, fig. 5) has a northwest peak oriented 329°, suggesting that the orientation of in situ stress may change, becoming more westerly away from the Sabine Uplift, toward the East Texas Basin.

The results reported by Komar and others (1971) are approximately the opposite of observations from the study area. Komar and others observed vertical fractures in the subsurface subparallel to lineaments but nearly perpendicular to surface fractures. In the study area, subsurface fractures are near-perpendicular to the northwest lineament direction and are subparallel to the trend of normal faults at the surface (Laubach and others, 1987). Furthermore, the perpendicular relationship between lineaments and subsurface fractures is the reverse of the parallelism between joints and fractures reported by Hickman and others (1985).

Maps of lineaments (fig. 3) were compared with maps of surface geology (fig. 8) to determine whether lineaments and surficial geologic features, such as faults and formation contacts, are parallel or coincident. This comparison revealed that, locally, parallelism exists between lineaments and some Eocene formation contacts. Likewise, some lineaments and faults are parallel.

The lineament map (fig. 3) also was compared with a subsurface structure map (fig. 9). No consistent relationship between structure and lineament orientation was discovered. Orientations of lineaments relative to slope on the base of the Austin Group range from parallel to perpendicular.

The lineament map (fig. 3) was divided into subsets using the 500-ft contours on a subsurface structure map on the base of the Austin Group (fig. 9). Bernshtein accuracy criteria for lineaments within these subsets were defined as described in the section on compilation of orientation data. The purpose of this procedure was to determine if orientations of the lineaments over different parts of the Sabine Uplift are affected by the orientation of the slope on the uplift or if the orientation of lineaments over the uplift is significantly different from that of lineaments elsewhere.

This analysis shows that the orientation of the slope of the Sabine Uplift, measured on the base of the Austin Group, has no systematic effect on the orientation of lineaments (fig. 10). The northwestern azimuth of H values for lineaments on the western side of the uplift (325°, fig. 10a), where the slope dips approximately due west (fig. 9, Subset A), is statistically equivalent to the northwest-trending peak of lineaments on the southwestern side of the uplift (323°, fig. 10b), where the slope dips approximately due south (fig. 9, Subset B). The northeastern azimuths for the same data sets are significantly different (fig. 10a, b) but show no correlation with slope on the underlying uplift. Similarly, when Subsets A and B are combined (fig. 10c) and compared with lineaments adjacent to the uplift (fig. 10d), the lineament peaks are significantly different. However, the orientations are not

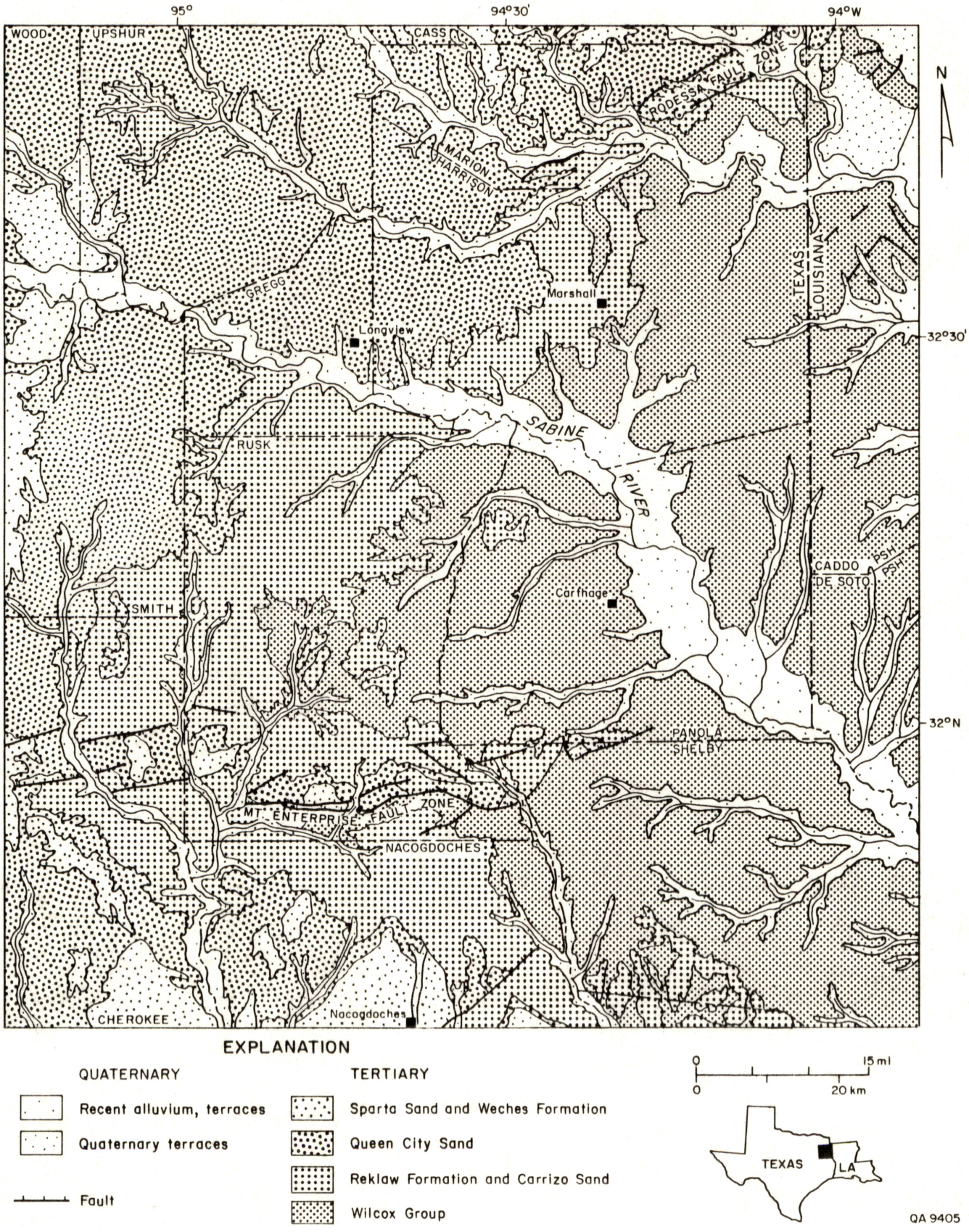

Figure 8. Geologic map of study area. Modified from Shelby and others (1967), Pieper and others (1975), and Louisiana Geological Survey (1984).

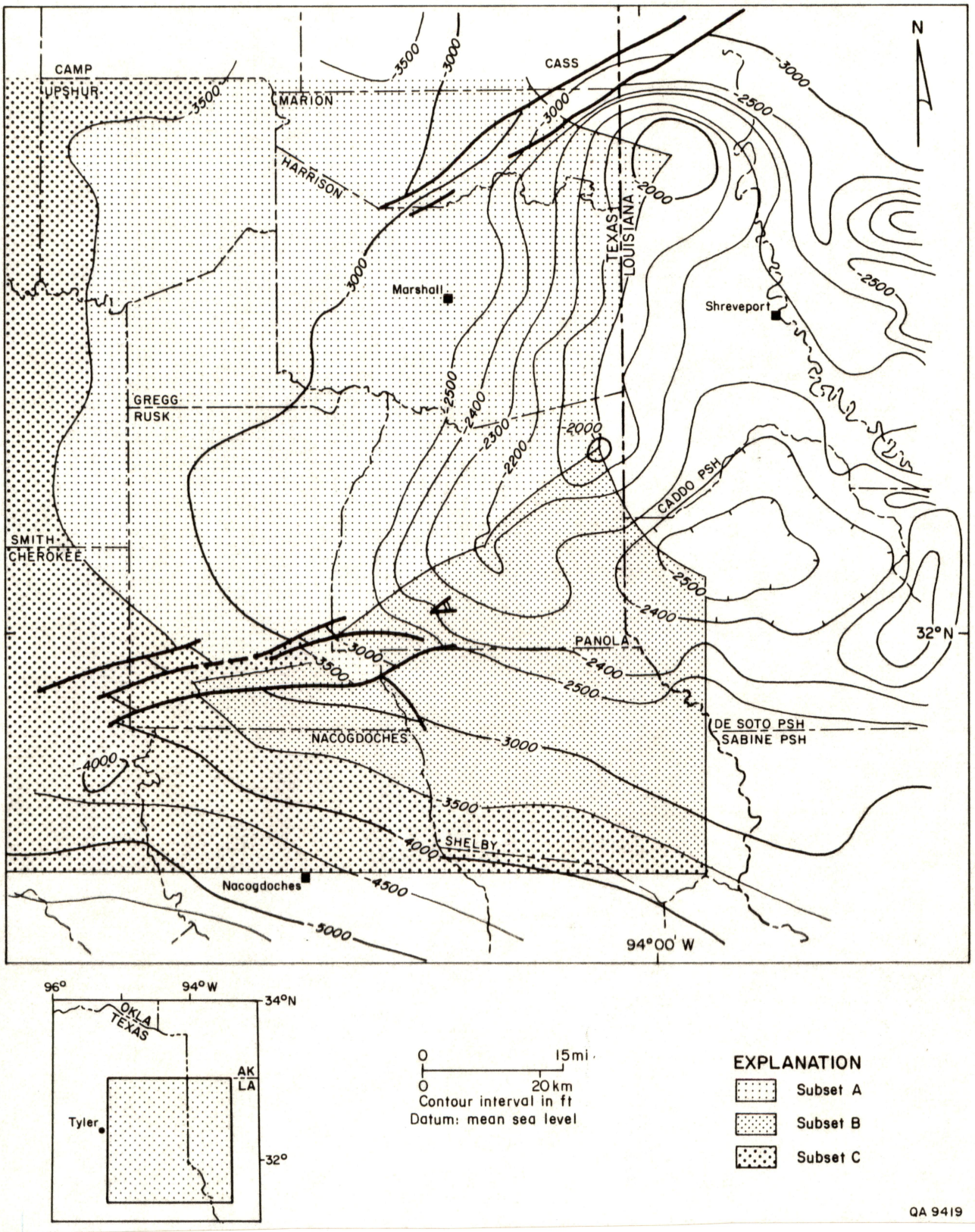

Figure 9. Structure-contour map on the base of the Austin Group. Subset letters refer to polar plots on figure 10. Modified from Jackson (1987, fig. 26).

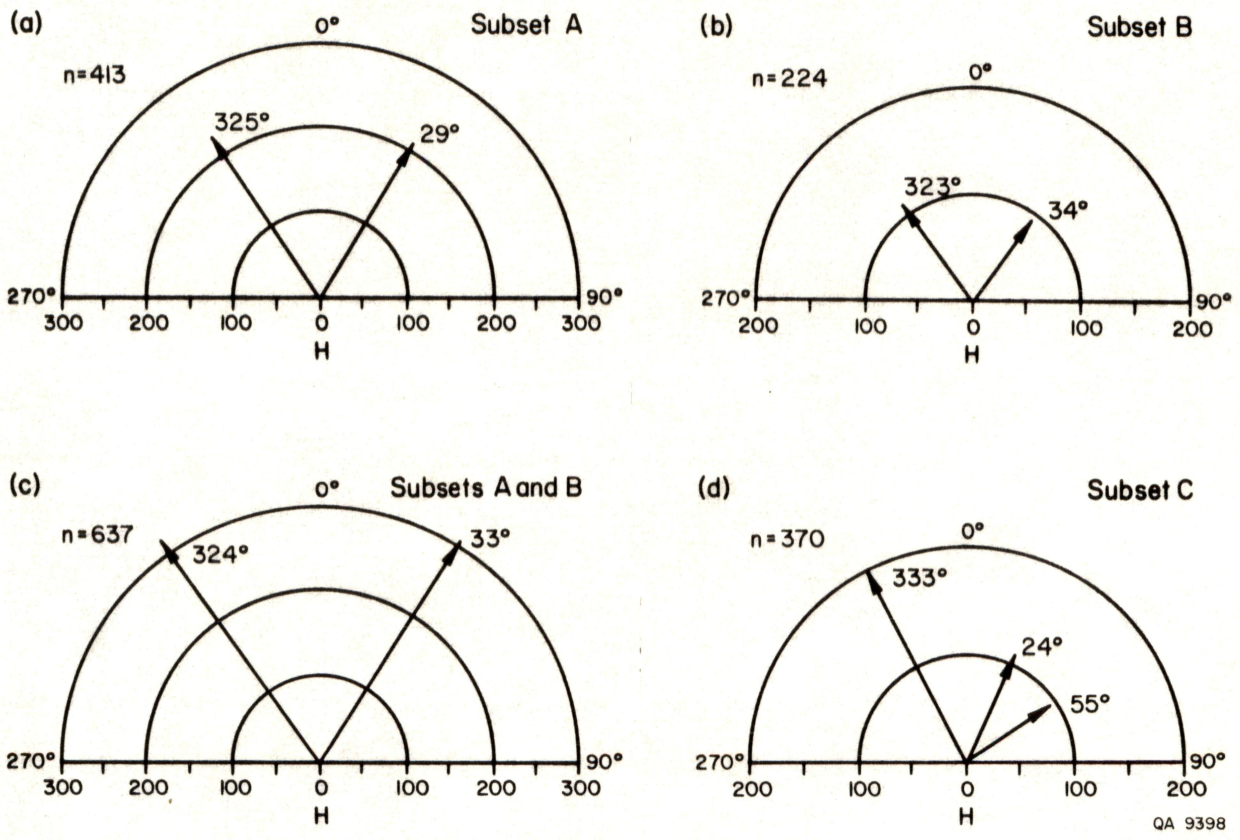

Figure 10. Polar plots of Bernshtein accuracy criterion (H) for subsets of lineaments in study area. See figure 9 for locations of subsets. (a) Subset A, western Sabine Uplift. (b) Subset B, southwestern Sabine Uplift. (c) Subsets A and B combined. (d) Subset C, adjacent to Sabine Uplift, below -3,500 ft elevation, as measured on the base of the Austin Group.

systematically shifted. The orientations of all other lineament peaks in separate subsets are significantly different from one another. For example, northeast-trending vectors for Subsets A, B, and C (fig. 10a, b, d) are all significantly different. But there is no apparent correlation between the orientations of lineament trends and slope of the Sabine Uplift.

Lineament Density and Geologic Structure

Some correlation between lineament density (fig. 11) and surface geology (fig. 8) was detected. Forty-eight percent of high density values ($\geq$16 km/100 km^2) are found in areas of Sparta and Weches outcrop, which cover only about 12 percent of the study area. Conversely, only 6 percent of the high values occur in areas of Quaternary alluvium, which covers about 16 percent of the study area. These relatively young deposits are mostly too unconsolidated to develop linear topographic features. Faults on surface geologic maps of the area are shown as concealed features where they cross Quaternary sediments (Shelby and others, 1967, and Pieper and others, 1975). No high density values are found in areas of Reklaw outcrop, which accounts for about 11 percent of the surface area in the study. Thus, the distribution of high values is clearly influenced by surficial geology.

No consistent spatial correspondence is evident between lineament density and the Sabine Uplift. Comparing the lineament density map (fig. 11) with subsurface structure (fig. 9) reveals no clear-cut correlation between high lineament density values and faults or slopes on the base of the Austin Group.

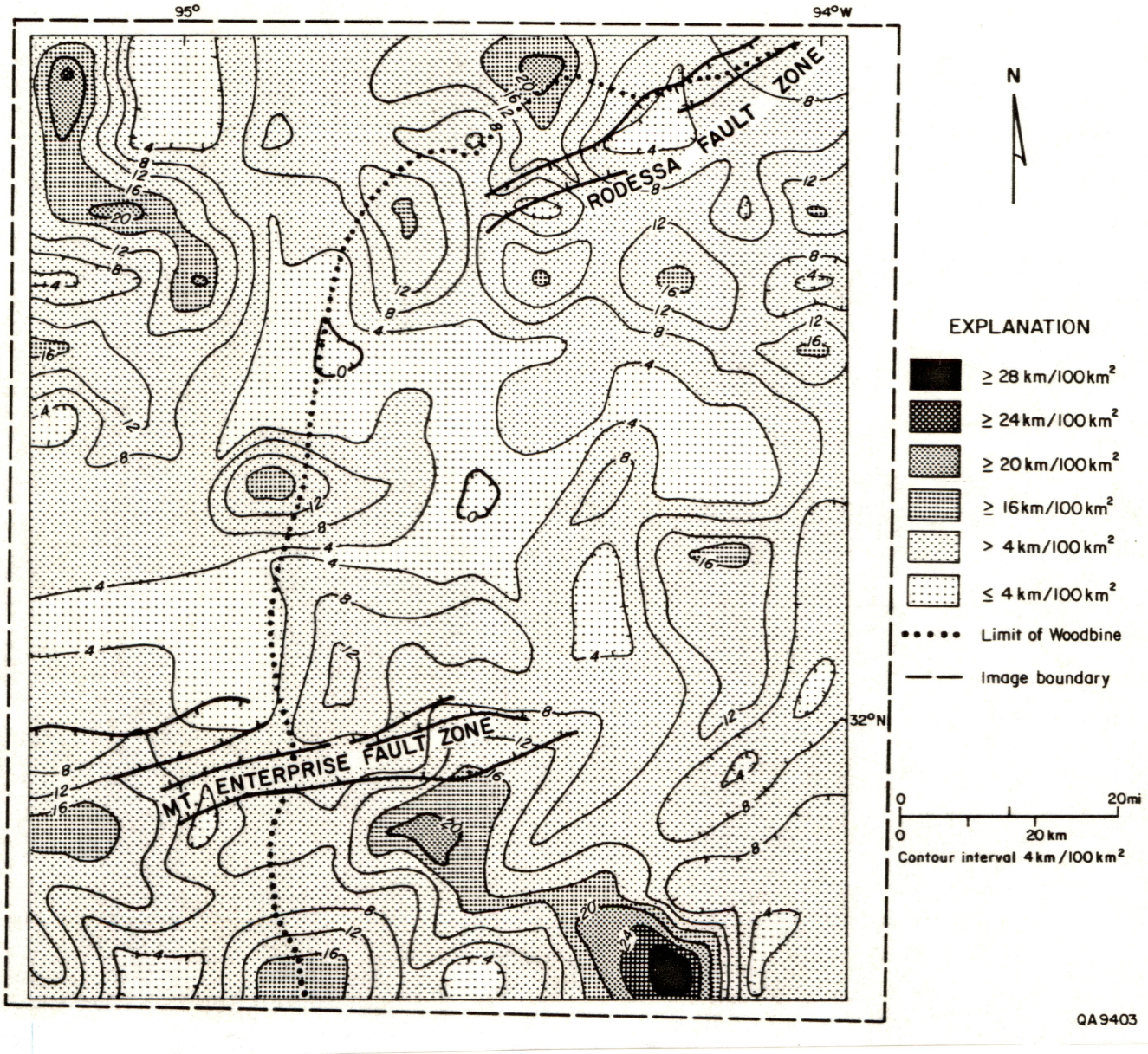

Figure 11. Map of radar lineament density. Dashed line corresponds to outer edges of radar images shown in figure 1.

DISCUSSION

The near-parallelism between northwest-trending borehole elongations and minimum principal horizontal stress measured by other means fits the model for stress-induced borehole breakouts (Gough and Bell, 1982; Plumb and Cox, 1987). It is reasonable to conclude that the northwest-oriented elliptical boreholes are functions of the regional extensional stress regime. The northwest-trending lineament peak in this study is parallel to wellbore elongations in the Jurassic Schuler Formation. Azimuth for the northwest-trending radar lineament peak is 325°. The orientation of horizontal least principal stress in the Cretaceous Travis Peak Formation ranges from 344° to 357°, depending on the method used to determine it. The mean northwest lineament orientation is significantly different from, but subparallel to, this trend of horizontal least principal stress in the Travis Peak. The reason for parallelism between minimum stress in the deeper formation and surface lineaments is unknown.

The northeast-trending radar lineament peak at 37° is not parallel to any known stress or fracture orientation. It is almost perpendicular (72°) to the northwest lineament peak. It may be an artifact of preferential radar shadowing of valley walls at angles from 8° to 39°.

Lineament density appears to be influenced by surficial geology rather than by geologic structures in the subsurface. This may be a result of the higher resolution of the SAR data, compared with that of Landsat data. The linear features detected on SAR data are shorter (table 1) than Landsat lineaments and are more easily confused with man-made features (table 3). They may be functions of surficial or near-surface processes, such as erosion, that have little to do with subsurface geologic structure or in situ stress. Nevertheless, similar predominant orientations were observed on SAR and Landsat data.

CONCLUSIONS

Radar lineaments have two significant orientation peaks: 325° and 37°. The northwest peak is subparallel to, but significantly different from, the orientation of least principal stress in the Travis Peak Formation. It is parallel to and statistically equivalent to mean orientation of wellbore elongations in the underlying Schuler Formation. The northeast peak apparently is not related to the stresses or fractures that have caused borehole elongation in the subsurface. These results indicate that radar lineaments in East Texas can be used to infer only the general orientation of minimum horizontal stress. Consequently, they probably cannot be used to independently predict the orientation of subsurface fractures. Locally, lineaments are parallel to faults and formation contacts. Orientations of individual lineaments have no consistent relationship with direction of slope on the Sabine Uplift. Lineament density has some correspondence with surface geology in that (1) no high values occur over Quaternary deposits and (2) almost half of the high density values are found on Sparta and Weches outcrops, which occupy only 12 percent of the study area. There is no spatial correspondence between lineament density and the Sabine Uplift. Radar lineaments are not reliable indicators of subsurface structural slope on the Sabine Uplift.

ACKNOWLEDGMENTS

The author wishes to acknowledge the cooperation of S. E. Laubach, E. R. Hunt of ResTech, Inc., and E. R. Monson of CER Corporation, who provided data used to determine orientations of in situ stress. Support staff at the Bureau of Economic Geology accomplished the vital steps required to turn research into report. Michelle Gilson was the editor, and Lana Dieterich coordinated production of the report. Figures were drafted by Annie Kubert-Kearns, James P. Nieto, and Maria E. Saenz

under the supervision of Richard L. Dillon. Word processing was by Anke Rommerskirch under the supervision of Lucille C. Harrell. Additional word processing was by Melissa Snell. This work was funded under Gas Research Institute Contract No. 5082-211-0708, R. J. Finley and S. P. Dutton, Co-Principal Investigators.

REFERENCES

Bailey, G. B., Dwyer, J. L., Francica, J. R., and Feng, M. S., 1984, Update on the use of remote sensing in oil and gas exploration, in Davidson, M. J., and Gottlieb, B. M., eds., Unconventional methods in exploration for petroleum and natural gas III, Symposium: Dallas, Texas, Southern Methodist University, p. 231-253.

Baumgardner, R. W., Jr., 1987, Landsat-based lineament analysis of the East Texas Basin and Sabine Uplift: The University of Texas at Austin, Bureau of Economic Geology Report of Investigations No. 167, 26 p.

Baumgardner, R. W., Jr., and Meador, K. J., 1987, Analysis of fracturing and wellbore elongation based on borehole televiewer, formation microscanner, and ellipticity logs, in Laubach, S. E., Baumgardner, R. W., Jr., and Meador, K. J., Analysis of natural fractures and borehole ellipticity, Travis Peak Formation, East Texas: The University of Texas at Austin, Bureau of Economic Geology, topical report prepared for Gas Research Institute under contract no. 5082-211-0708, 128 p.

Berger, Zeev, 1982, The use of Landsat data for detection of buried and obscured geologic structures in the East Texas Basin, U.S.A.: Proceedings, International Symposium on Remote Sensing of Environment, Second Thematic Conference, Remote Sensing for Exploration Geology, Ft. Worth, Texas, p. 579-589.

Brown, R. O., Forgotson, J. M., and Forgotson, J. M., Jr., 1980, Predicting the orientation of hydraulically created fractures in the Cotton Valley Formation of East Texas: Society of Petroleum Engineers of AIME, 55th Annual Fall Conference, Dallas, Texas, Paper SPE 9269, 12 p.

Cannon, P. J., 1982, Quantitative evaluation of the information levels from radar imagery for geologic exploration: Proceedings, International Symposium on Remote Sensing of Environment, Second Thematic Conference, Remote Sensing for Exploration Geology, Ft. Worth, Texas, v. 1, p. 355-363.

Cheeney, R. F., 1983, Statistical methods in geology: Boston, George Allen and Unwin, 169 p.

Davis, J. C., 1986, Statistics and data analysis in geology, (2d ed.): New York, John Wiley and Sons, 646 p.

Dix, O. R., and Jackson, M. P. A., 1981, Statistical analysis of lineaments and their relation to fracturing, faulting, and halokinesis in the East Texas Basin: The University of Texas at Austin, Bureau of Economic Geology Report of Investigations No. 110, 30 p.

Gough, D. I., and Bell, J. S., 1982, Stress orientations from borehole wall fractures with examples from Colorado, East Texas, and northern Canada: Canadian Journal of Earth Sciences, v. 19, no. 7, p. 1358-1370.

Grout, M. A., and Verbeek, E. R., 1985, Fracture history of the Plateau Creek and adjacent Colorado River valleys, southern Piceance Basin: implications for predicting joint patterns at depth: U. S. Geological Survey Open-File Report 85-744, 17 p.

Hickman, S. H., Healy, J. H., and Zoback, M. D., 1985, In situ stress, natural fracture distribution, and borehole elongation in the Auburn geothermal well, Auburn, New York: Journal of Geophysical Research, v. 90, no. B7, p. 5497-5512.

INTERA Technologies, 1985, Side-looking airborne radar (SLAR) data acquisition, spring of 1985, technical proposal: Houston, unpublished report RP85-010, 34 p.

Jackson, M. L. W., 1987, Mesozoic and Cenozoic structural history of the Sabine Uplift area, East Texas, in Baumgardner, R. W., Jr., and Jackson, M. L. W., Landsat-based lineament analysis, East Texas Basin, and structural history of the Sabine Uplift area, East Texas and North Louisiana: The University of Texas at Austin, Bureau of Economic Geology, topical report prepared for the Gas Research Institute under contract no. 5082-211-0708, 119 p.

Jeffrey, R. G., Skach, E. W., Nimerick, K., and Redmond, J., 1987, Rock mechanics testing of core samples from staged field experiment well Howell No. 5: contract report prepared for the Gas Research Institute by Dowell-Schlumberger, 42 p.

Komar, C. A., Overbey, W. K., Jr., Rough, R. L., and Lambert, W. G., 1971, Factors that predict fracture orientation in a gas storage reservoir: Journal of Petroleum Technology, v. 23, May, p. 546-550.

Laubach, S. E., Baumgardner, R. W., Jr., and Meador, K. J., 1987, Analysis of natural fractures and borehole ellipticity, Travis Peak Formation, East Texas: The University of Texas at Austin, Bureau of Economic Geology, topical report prepared for the Gas Research Institute under contract no. 5082-211-0708, 128 p.

Louisiana Geological Survey, 1984, Geologic map of Louisiana: scale 1:500,000.

MacDonald, H. C., Kirk, J. N., Dellwig, L. F., and Lewis, A. J., 1969, The influence of radar look-direction on the detection of selected geological features: Proceedings, Sixth International Symposium on Remote Sensing of Environment, University of Michigan, Ann Arbor, v. 1, p. 637-650.

Owen, L. B., Toronto, T. W., and Sinha, K. P., 1987, Final report--strain recovery measurements, Howell No. 5 well: Terra Tek Research, submitted to CER Corporation, Las Vegas, Nevada, TR87-58.

Peake, W. H., and Oliver, T. L., 1971, The response of terrestrial surfaces at microwave frequencies: Columbus, Ohio, Ohio State University Electroscience Laboratory, 2440-7, Technical Report AFAL-TR-70-301.

Pieper, M. K., Haenggi, W. T., and Wright, A. C., 1975, Tyler sheet: The University of Texas at Austin, Bureau of Economic Geology Geologic Atlas of Texas, scale 1:250,000.

Plumb, R. A., and Cox, J. W., 1987, Stress directions in eastern North American determined to 4.5 km from borehole elongation measurements: Journal of Geophysical Research, v. 92, no. B6, p. 4805-4816.

Plumb, R. A., and Hickman, S. H., 1985, Stress-induced borehole elongation: a comparison between the four-arm dipmeter and the borehole televiewer in the Auburn geothermal well: Journal of Geophysical Research, v. 90, no. B7, p. 5513-5521.

Sabins, F. F., Jr., 1986, Remote sensing principles and interpretation (2d ed.): New York, W. H. Freeman and Co., 449 p.

Shelby, C. A., Pieper, M. K., and Wright, A. C., 1967, Palestine sheet: The University of Texas at Austin, Bureau of Economic Geology Geologic Atlas of Texas, scale 1:250,000.

Strubhar, M. K., Fitch, J. L., and Glenn, E. E., Jr., 1975, Multiple, vertical fractures from an inclined wellbore--a field experiment: Journal of Petroleum Technology, v. 27, May, p. 641-647.

Tillman, J. E., 1983, Exploration for reservoirs with fracture-enhanced permeability: Oil and Gas Journal, v. 8, no. 8, p. 165-180.

Trevett, J. W., 1986, Imaging radar for resources surveys: New York, Chapman and Hall, 313 p.

Verbeek, E. R., and Grout, M. A., 1984, Prediction of subsurface fracture patterns from surface studies of joints--an example from the Piceance Creek Basin, Colorado, in Spencer, C. W., and Keighin, C. W., eds., Geologic studies in support of the U. S. Department of Energy Multiwell Experiment, Garfield County, Colorado: U. S. Geological Survey Open-File Report 84-757, p. 75-86.

Vistelius, A. B., 1966, Structural diagrams: New York, Pergamon Press, 178 p.

Wise, D. U., 1969, Pseudo-radar topographic shadowing for detection of sub-continental sized fracture systems: Proceedings, Sixth International Symposium on Remote Sensing of Environment, University of Michigan, Ann Arbor, v. 1, p. 603-615.

Woodruff, C. M. and Caran, S. C., 1984, Lineaments of Texas--possible surface expressions of deep-seated phenomena: The University of Texas at Austin, Bureau of Economic Geology, final report prepared for United States Department of Energy, Division of Geothermal Energy, under contract no. DE-AS07-79ID12057, 68 p.

Yamaguchi, Yasushi, 1985, Image-scale and look-direction effects on the detectability of lineaments in radar images: Remote Sensing of Environment, v. 17, no. 2, p. 117-127.

Zoback, M. D., Moos, D., Mastin, L., and Anderson, R. N., 1985, Well bore breakouts and in situ stress: Journal of Geophysical Research, v. 90, no. B7, p. 5523-5530.

Zoback, M. L., and Zoback, Mark, 1980, State of stress in the conterminous United States: Journal of Geophysical Research, v. 85, no. B11, p. 6113-6156.